

Treatment of Pancreatic Cancer Cells with Dicumarol Induces Cytotoxicity and Oxidative Stress

Anne Lewis,⁴ Matthew Ough,⁴ Ling Li,²
Marilyn M. Hinkhouse,⁵ Justine M. Ritchie,³
Douglas R. Spitz,^{2,3} and Joseph J. Cullen^{1,2,3,4,5}

Departments of ¹Surgery, ²Radiation Oncology and ³Holden Comprehensive Cancer Center, and ⁴University of Iowa College of Medicine, Iowa City, Iowa, and ⁵Veterans Affairs Medical Center, Iowa City, Iowa

ABSTRACT

Purpose: NAD(P)H:quinone oxidoreductase (NQO₁) catalyzes the two-electron reduction of quinones to hydroquinones. This reaction is believed to prevent the one-electron reduction of quinones that would result in redox cycling with generation of superoxide (O₂⁻). We have recently demonstrated that inhibition of NQO₁ with dicumarol increases intracellular O₂⁻ production and inhibits the *in vitro* malignant phenotype of pancreatic cancer cells (J. Cullen *et al.*, *Cancer Res.*, 63: 5513–5520, 2003). We hypothesized that inhibition of NQO₁ would increase cell killing, induce oxidative stress, and inhibit *in vivo* tumor growth.

Experimental Design and Results: In the human pancreatic cancer cell line MIA PaCa-2, dicumarol decreased cell viability, as measured by the 3-(4,5-dimethylthiazol-2-yl)-2,5-diphenyltetrazolium bromide assay and decreased clonogenic survival. Dicumarol increased the percentage of apoptotic cells in a time-dependent and dose-dependent manner as measured by 3,3'-diaminobenzidine staining and flow cytometry, which was associated with cytochrome *c* release and poly(ADP-ribose) polymerase cleavage. Dicumarol also induced oxidative stress as evidenced by increased total glutathione and oxidized glutathione, as well as sensitizing to cell killing mediated by menadione. In established orthotopic pancreatic tumors in nude mice, intratumoral injections of dicumarol slowed tumor growth and extended survival.

Conclusions: Inhibition of NQO₁ with dicumarol induces cell killing and oxidative stress in pancreatic cancer cells and speculate that dicumarol may prove to be useful in pancreatic cancer therapeutics.

INTRODUCTION

3,3'-Methylenebis[4-hydroxycoumarin] (dicumarol) is a naturally occurring anticoagulant derived from coumarin, which is obtained from sweet clover (*Melilotus alba*; Refs. 1, 2). Coumarin, the parent molecule of dicumarol, and a variety of coumarin compounds have demonstrated numerous antitumor and antiproliferative effects. Coumarin compounds have been shown to inhibit proliferation of particular human malignant cell lines *in vitro* (3–8), as well as affecting tumor activity against several *in vivo* tumor types (1, 9–13). In clinical trials, these compounds have also been demonstrated to have some activity against prostate cancer, malignant melanoma, and metastatic renal cell carcinoma (14–16). Additionally, dicumarol studies have found decreased metastases in animal models (17). Although such coumarin compounds as dicumarol have been used in cancer therapy, little is known about the mechanism of action of these drugs.

Dicumarol has a number of effects that may lead to inhibition of cell proliferation. Dicumarol inhibits reductases, including NAD(P)H:quinone oxidoreductase (NQO₁), by competing with NADH for the binding site of the oxidized NQO₁ form (18). Inhibition of NQO₁ by dicumarol does not appear to involve vitamin K epoxide oxidoreductase or vitamin K metabolism because addition of vitamin K does not impair the growth-inhibiting effect of dicumarol in melanoma cells (19). The growth inhibitory effect of dicumarol also appears to be relatively specific for tumor cells because proliferation of normal human airway myocytes was not affected (19). It has been proposed that by preventing the two-electron reduction of quinones, dicumarol increases the oxidative stress within the cell via the buildup of semiquinones, which leads to increased cell toxicity (20–22). Other hypotheses have been proposed as well. Madari *et al.* (1) suggest coumarin compounds interfere with spindle microtubule function during mitosis, thus inhibiting cell proliferation.

Recent studies from our laboratory suggest that inhibiting NQO₁ with dicumarol would suppress the malignant phenotype of pancreatic cancer cells known to overexpress this enzyme (23). Reverse transcription-PCR, Western blots, and activity assays demonstrated that NQO₁ was up-regulated in the pancreatic cancer cell lines tested but present in very low amounts in the normal human pancreas. These studies demonstrate that NQO₁ is up-regulated in pancreatic cancer cell lines, which is consistent with previous studies that have shown that expression of NQO₁ is up-regulated in tumors of the liver, lung, colon, breast, and pancreas compared with normal tissues of the same origin (24, 25). Additionally, in cells that lack functional mitochondria, activity of this plasma membrane oxidoreductase system is greatly up-regulated to support cell growth (26). Previous investigations have hypothesized that NQO₁ is up-regulated in various tumors to accommodate the needs of rapidly metabolizing cells to regenerate NAD⁺ (8).

Received 12/3/03; revised 2/26/04; accepted 3/3/04.

Grant support: NIH Grants DK 60618, CA 66081, DE-FG02-02ER63447, and HL07485-24 and the Medical Research Service, Department of Veterans Affairs.

The costs of publication of this article were defrayed in part by the payment of page charges. This article must therefore be hereby marked *advertisement* in accordance with 18 U.S.C. Section 1734 solely to indicate this fact.

Requests for reprints: Joseph J. Cullen, 4605 JCP, University of Iowa Hospitals and Clinics, Iowa City, IA 52242. Phone: (319) 353-8297; Fax: (319) 356-8378; E-mail: joseph-cullen@uiowa.edu.

To determine whether inhibition of NQO₁ would alter the malignant phenotype, MIA PaCa-2-pancreatic cancer cells were treated with a selective inhibitor of NQO₁, dicumarol (23). Dicumarol increased intracellular production of O₂⁻, as measured by hydroethidine staining, and inhibited cell growth. Both of these effects (cell growth inhibition and hydroethidine staining) were blunted with infection of an adenoviral vector containing the cDNA for manganese superoxide dismutase. Dicumarol also inhibited plating efficiency and growth in soft agar. Thus, inhibition of NQO₁ with dicumarol offers a potential therapeutic strategy directed against pancreatic cancer by altering the superoxide production in pancreatic cancer cells. Observations consistent with these findings were also obtained by Li *et al.* who demonstrated inhibition of NAD(P)H oxidase with iodonium compounds, including diphenyleneiodonium, resulted in increased mitochondrial O₂⁻ production leading to apoptosis (27). Diphenyleneiodonium, which inhibits flavoenzymes such as NQO₁, also increased ethidium fluorescence in HL-60 cells, and the diphenyleneiodonium-induced generation of O₂⁻ was reduced by overexpression of manganese superoxide dismutase. Although previous studies in rat liver have demonstrated that the bulk of NQO₁ is located in the cytoplasm, lesser amounts are present in the mitochondria (28). The cellular distribution of NQO₁ in rapidly dividing tumor cells is variable (29). However, these previous results suggested that increasing mitochondrial superoxide production by inhibiting NQO₁ could prove to be a useful mechanism in treating cancer cells that overexpress NQO₁.

In the current study, we hypothesize that the effect of dicumarol on pancreatic cancer cells is caused by a cytotoxic mechanism involving oxidative stress, and this could prove effective as an antitumor agent *in vivo*. The results demonstrate that dicumarol induces a dose-dependent and time-dependent cytotoxicity as demonstrated by increased clonogenic cell death, increased apoptosis, cytochrome *c* release, and poly(ADP-ribose) polymerase (PARP) cleavage, which is associated with increases in parameters of thiol metabolism that are indicative of oxidative stress. Additionally, in preestablished pancreatic malignancies in nude mice, intratumoral injections of dicumarol led to decreased tumor volume and increased animal survival.

MATERIALS AND METHODS

Cell Culture. MIA PaCa-2 cells were purchased from American Type Culture Collection (Manassas, VA) and are human primary pancreatic adenocarcinoma cells derived from tumor tissue of the pancreas obtained from a 65-year-old male. The cell cultures were maintained at 37°C in DMEM (Life Technologies, Inc., Grand Island, NY) supplemented with 10% heat-inactivated fetal bovine serum and 2.5% horse serum.

Cell Homogenization and Protein Determination. Cells were washed three times in PBS (pH 7.0), scraped from the dishes using a rubber policeman, and then collected in phosphate buffer (pH 7.8). This was followed by sonic disruption on ice for 30 s in 10-s bursts using a VibraCell sonicator (Sonics and Materials, Inc., Danbury, CT) at 100% power. Protein concentration was determined using the Bio-Rad Bradford dye binding protein assay kit (Hercules, CA) according to the manufacturer's instructions.

Western Blotting. Whole cell extracts were prepared by direct lysis of scraped, PBS-washed cells (both floating and attached cells were pooled) in buffer composed of 6 M urea, 2% SDS, 10% glycerol, 62.5 mM Tris-HCl (pH 6.8), 5% β-mercaptoethanol, and 5 μg/ml bromophenol blue followed by sonication. Equal amounts of protein were heated at 65°C for 10 min and loaded into each lane of a 12.5% polyacrylamide gel with a 5% stacking gel. After electrophoresis, proteins were then electrotransferred to nitrocellulose sheets. Loading equivalence was monitored by Ponceau S staining of the membrane. To prepare cytosolic extracts for the cytochrome *c* Western blot, cell pellets from control or dicumarol-treated cells were suspended in 600 μl of extraction buffer [220 mM mannitol, 68 mM sucrose 50 mM HEPES-KOH (pH 7.4), 50 mM KCl, 5 mM EGTA, 2 mM MgCl₂, 1 mM DTT, and protease inhibitors). After 30 min of incubation on ice, cells were homogenized with a glass dounce and a B pestle (40 strokes). Cell homogenates were spun at 14,000 × *g* for 15 min. The supernatants (cytosolic fraction) were stored at -80°C until ready for Western blotting. Cytochrome *c* antibody (1:1000 dilution) and the anti-PARP antibody (1:1000 dilution) were purchased from BD PharMingen (San Diego, CA). The blots were incubated with goat-antimouse IgG-horseradish peroxidase secondary antibody (Santa Cruz Biotechnology, Santa Cruz, CA; 1:2000) for 2 h at room temperature. The washed blot was then treated with enhanced chemiluminescence Western blot detection solution (Amersham Life Science, Buckinghamshire, United Kingdom) and exposed to X-ray film. All Western blots were performed in triplicate.

Cell Viability. As an indicator of cell metabolic viability, the 3-(4,5-dimethylthiazol-2-yl)-2,5-diphenyltetrazolium bromide assay was used. Cells were seeded at 1 × 10⁴ in a 96-well plate in full media. 3-(4,5-Dimethylthiazol-2-yl)-2,5-diphenyltetrazolium bromide (5 mg/ml) was added to the wells and incubated at 37°C for 3 h. Lysing buffer, consisting of 20% SDS in a 1:1 solution of DMF (*N,N*-dimethyl formamide), was added and incubated at 37°C for 16 h. The plate was read at 590 nm on an Ultramark microplate imaging system (Bio-Rad, Hercules, CA).

Clonogenic Assay. MIA PaCa-2 cells (5 × 10³) were treated with dicumarol (0, 50, 100, or 250 μM) for 4, 24, or 48 h. For survival determination, cells were trypsinized and plated for clonogenic cell survival assay. After 1 week of incubation at 37°C, colonies > 50 cells were stained and counted. The percent survival was determined using the following equation: percentage of survival = (colonies formed/cells seeded) × 100.

Measurement of Apoptosis. Degradation of DNA was measured by flow cytometry using propidium iodide (PI). Cells were collected and fixed in suspension in 70% ethanol on ice and then stored at -20°C. Cells were centrifuged at 500 × *g*, washed with 5 ml of HBSS, centrifuged again, and resuspended in 1 ml of HBSS. After addition of 0.2 ml of phosphate citrate buffer (pH 7.8), cells were incubated at room temperature for 5 min before being washed again and resuspended in HBSS containing 20 μg/ml PI and 10 μg/ml RNase A. After 30 min incubation in the dark at room temperature, PI fluorescence was analyzed by flow cytometry.

In addition to PI fluorescence and as another independent measurement of apoptosis, we measured 3,3'-diaminobenzidine (DAB) staining in MIA PaCa-2 cells with and without dicum-

arol treatment. Cells were fixed in 10% buffered formalin for 15 min and then stored in PBS. Proteinase K (TACs 2 TdT DAB kit; Trevigen, Gaithersburg, MD; 50 μ l/slide) was applied to each slide for 15 min and then rinsed. Slides were placed in 10% hydrogen peroxide in methanol for five min and were rinsed in PBS for one min. Slides were then placed in 10% terminal deoxynucleotidyltransferase (TdT)-labeling buffer for 5 min. The slides were then incubated for one h at 37°C in a solution of 50 μ l of TdT-labeling buffer, 1 μ l of TdT enzyme, 1 μ l of Mn^{2+} stock, and 1 μ l of TdT deoxynucleoside triphosphate/slide. Slides were then agitated for 15 s in TdT stop buffer and soaked for 5 min. The slides were rinsed in PBS and then Strep-HRP solution (Jackson ImmunoResearch Laboratories, West Grove, PA; 50 μ l of PBS + 1 μ l of Strep-HRP/slide) was applied for 10 min, and the slides were rinsed in PBS for 2 \times 2 min. DAB was applied, and the slides were washed and then counterstained with methyl green. The slides were fixed, mounted, and stored in the dark. Slides were viewed at \times 40 on the Olympus BX-51 light microscope, and samples were photographed using SPOT software program.

Thiol Analysis. Cells were washed with ice-cold PBS, scraped into cold PBS, and centrifuged at 4°C for 5 min at 400 \times g to obtain cell pellets that were then frozen at -80°C. Pellets were thawed and homogenized in 50 mM potassium phosphate buffer (pH 7.8) containing 1.34 mM diethylenetriaminepentaacetic acid. Total glutathione content [reduced glutathione + glutathione disulfide (GSSG)] was determined by the method of Anderson (30). GSSG was distinguished by the addition of 2 μ l of a 1:1 mixture of 2-vinylpyridine and ethanol/30 μ l of sample followed by incubation for 1.5 h and assayed as previously described by Griffith (31). All biochemical determinations were normalized to the protein content of whole homogenates using the method of Lowry *et al.* (32).

Nude Mice. Thirty-day-old athymic nude mice were obtained from Harlan Sprague Dawley (Indianapolis, IN). The nude mice protocol was reviewed and approved by the Animal Care and Use Committee of the University of Iowa on January 9, 2003. The animals were housed four to a cage and fed a sterile commercial stock diet and tap water, *ad libitum*. Animals were allowed to acclimate in the unit for 1 week before any manipulations were performed. Each experimental group consisted of four to six mice.

Intratumoral Injections of Dicumarol in Established Pancreatic Tumor Heterotopic Xenografts. MIA PaCa-2 tumor cells (2×10^6) were delivered s.c. into the flank region of nude mice from a 1-ml tuberculin syringe equipped with a 25-gauge needle. In the *in vivo* study, tumors were allowed to grow between 28 and 56 mm³ (15 days), at which time, they were treated with varying doses of dicumarol (0, 50, 100, or 250 μ M). Dicumarol was delivered through one or two injection sites in the tumor, depending on tumor size at the time of injection. Dicumarol in sterile PBS (100 μ l total volume) was delivered to the tumor by means of a 25-gauge needle attached to a 1-ml tuberculin syringe. This was defined as day 1 of the experiment. Control tumors received 100 μ l of sterile PBS at the same time points. Tumor size was measured every 3 days by means of a vernier caliper, and tumor volume was estimated according to the following formula: tumor volume = $\pi/6 \times L \times W^2$, where L is the greatest dimension of the tumor, and W is the dimension

of the tumor in the perpendicular direction (33). Animals were killed by CO₂ asphyxiation when the tumors reached a predetermined size of 10 \times 10 mm, and this was considered the time to sacrifice.

Statistical Analysis. Statistical analysis for the *in vitro* studies was performed using SYSTAT. A single factor ANOVA, followed by posthoc Tukey test, was used to determine statistical differences between means. All means were calculated from three experiments, and error bars represent SE of mean (SE). All Western blots, activity assays, and activity gel assays were repeated at least twice.

To compare the treatment groups over time for tumor volume, the linear mixed model analysis (34), assuming either an autoregressive order 1 or compound symmetry covariance structure for within subjects, was used. Selection of the covariance structure was based on the Akaike's Information Criterion (35). In the linear mixed model analysis, group was considered a fixed effect, and day was considered a continuous. For the *in vivo* studies, tumor volume was compared among the four groups using the data from days 1 through 28. Survival curves were estimated by the Kaplan-Meier product limit curves. The log-rank test was used to compare survival between the groups. All data analyses for the *in vivo* data were done using SAS version 8.0.

RESULTS

Dicumarol Decreases Cell Viability and Clonogenic Survival. To determine cell metabolic viability, the 3-(4,5-dimethylthiazol-2-yl)-2,5-diphenyltetrazolium bromide assay was used. Previous studies have demonstrated that dicumarol is also extensively protein bound, which can complicate its use in cellular systems (36). Furthermore, the effective concentration of dicumarol that is required to inhibit NQO₁ depends on the efficiency of the second substrate or electron acceptor because of the competitive nature of dicumarol inhibition and the ping-pong kinetic mechanism of NQO₁ (37). Fig. 1A demonstrates that dicumarol decreases cell viability in a time-dependent and concentration-dependent manner. When compared with MIA PaCa-2 cells in full 10% serum that received the vehicle alone (0 μ M dicumarol), dicumarol resulted in decreased cell viability at the 100 and 250 μ M dose given for 48 and 72 h. For example, when cells received 100 and 250 μ M dicumarol in full serum for 48 and 72 h, there was a significant decrease in cell viability from 27 to 73% compared with controls ($P < 0.01$ versus 0 μ M dicumarol). Dicumarol also decreases cell viability in a serum-dependent manner (Fig. 1B). When compared with MIA PaCa-2 cells that were treated with dicumarol in full serum, cells treated in 2% had additional decreases in cell viability. When compared with MIA PaCa-2 cells receiving vehicle alone, dicumarol resulted in decreased cell viability at the 50 μ M dose for the 48 and 72 h time periods, decreased cell viability at 250 μ M 24, 48, and 72 h time points, and at the 100 μ M dose for all time periods (data not shown). For example, cells treated with dicumarol (100 μ M) for 48 h, cell viability decreased from 61 \pm 5% in full serum to 36 \pm 6% in 2% serum and, in cells treated at the same dose for 72 h, cell viability decreased from 73 \pm 8% in full

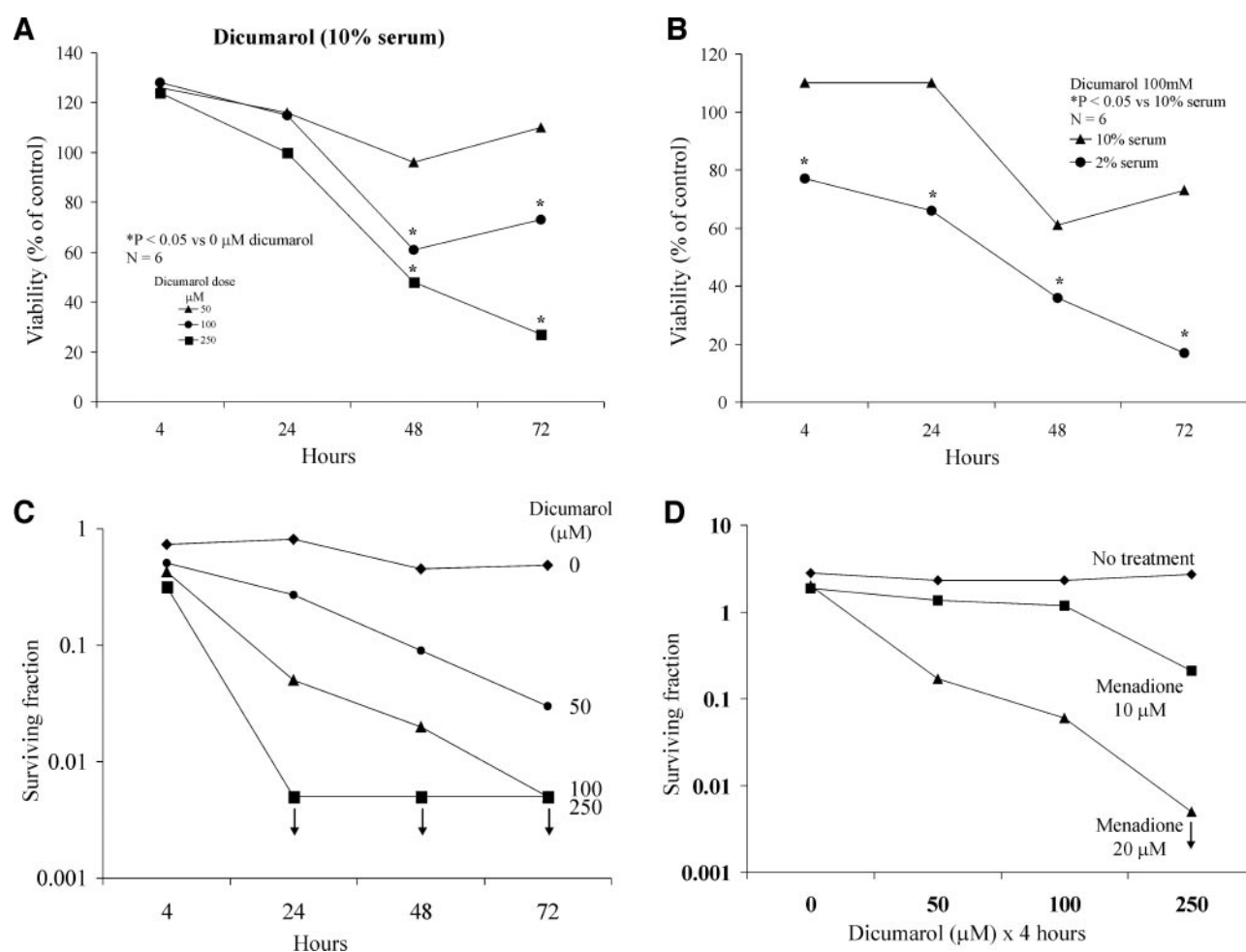


Fig. 1 A, dicumarol decreases cell viability in a time-dependent and dose-dependent manner as measured by 3-(4,5-dimethylthiazol-2-yl)-2,5-diphenyltetrazolium bromide assay. The absorbance of MIA-PaCa-2 cells treated with dicumarol (0–250 μ M) for 4, 24, 48, and 72 h, plated in full serum. Dicumarol resulted in decreased cell viability at the 100 and 250 μ M dose given for 48 and 72 h as determined by a microplate reader at 590 nm. Means, $*P < 0.05$ versus 0 μ M dicumarol, $n = 6$. B, dicumarol decreases cell viability in a time-dependent, dose-dependent, and serum-dependent manner as measured by 3-(4,5-dimethylthiazol-2-yl)-2,5-diphenyltetrazolium bromide assay. The absorbance of MIA-PaCa-2 cells treated with dicumarol (0–250 μ M) for 4, 24, 48, and 72 h, plated in 2% serum. Dicumarol resulted in decreased cell viability at the 48 and 72 h time periods, decreased cell viability at 250 μ M 24, 48, and 72 h time points, and at the 100 μ M dose for all time periods as determined by a microplate reader at 590 nm. Means, $*P < 0.05$ versus 0 μ M dicumarol, $n = 6$. C, dicumarol decreases pancreatic cancer clonogenic cell survival in a time-dependent and dose-dependent manner. A clonogenic assay was performed on MIA-PaCa-2 cells treated with dicumarol (0–250 μ M) for 4, 24, 48, and 72 h. The arrows on the 24-, 48-, and 72-h time points for the 250 μ M dicumarol group and on the 72-h time point for the 100 μ M indicate that no colonies were formed when 5000 cells were plated in the dishes and treated with dicumarol. Means, $n = 3$. D, menadione enhances dicumarol-induced clonogenic cell death. A clonogenic assay was performed on MIA-PaCa-2 cells treated with dicumarol (0–250 μ M) for 4 h with menadione (0, 10, and 20 μ M). The arrow on the time point for the dicumarol 250 μ M + menadione 20 μ M indicate that no colonies were formed when 5000 cells were plated in the dishes and treated with dicumarol. $*P < 0.05$ versus 0 μ M menadione, means, $n = 3$.

serum to $17 \pm 5\%$ in 2% serum (Fig. 1B; $P < 0.001$ versus full serum). Thus, the rest of the studies performed were done in 2% serum.

In another independent measure of the cytotoxicity of dicumarol on pancreatic cancer cells, clonogenic cell survival was decreased in a time-dependent and dose-dependent manner (Fig. 1C). With 24 h of treatment, all doses of dicumarol (50, 100, and 250 μ M) used had significantly decreased the surviving fraction of cells when compared with the control cells that received no treatment. In fact, in cells that were treated with 100 μ M dicumarol for 48 h or 250 μ M dicumarol for 24, 48, and 72 h,

there were no colonies present when the plates were stained and counted.

Using NAD(P)H, NQO₁ directly reduces quinones to hydroquinones, thus bypassing the reactive semiquinone intermediate. One potential mechanism for dicumarol toxicity is the inhibition of NQO₁ causing increases in reactive oxygen species production if steady-state levels of semiquinones increase and redox cycle to form superoxide (O₂⁻) and hydrogen peroxide (H₂O₂). Using this biochemical rationale, we hypothesized that increasing quinone concentration (with the exogenous addition of quinones) during exposure to dicumarol would increase pan-

creatic cancer cell killing. Cells treated with dicumarol (50, 100, and 250 μM for 4 h) or menadione (10 and 20 μM for 4 h) resulted in increased cytotoxicity when compared with dicumarol alone (Fig. 1D). Dicumarol (50, 100, and 250 μM) for 4 h had little effect on clonogenic cell survival. Likewise, menadione (10 and 20 μM for 4 h) had little effect on clonogenic survival. These results support the hypothesis that treatment with dicumarol enhances the cytotoxicity of quinones by inhibiting the conversion to hydroquinone.

Dicumarol Induces Apoptosis in MIA PaCa-2 Cells.

Apoptosis was studied by flow cytometry using PI and light microscopy with DAB staining. Treatment of MIA PaCa-2 cells

with 50, 100, and 250 μM dicumarol resulted in a dose-dependent and time-dependent increase in apoptosis as measured by flow cytometry (Fig. 2A). For example, there was a 6-fold increase in the sub- G_1 population of MIA PaCa-2 cells as measured by flow cytometry when treated with 100 and 250 μM dicumarol. As seen in Fig. 2B, cell cycle analysis was performed by flow cytometry, and apoptotic cells were estimated by calculating the number of subdiploid cells in the cell cycle histogram. The number of apoptotic cells correlated well with the results seen in the DAB staining (Fig. 2B). As demonstrated in the left panel, DAB staining is increased with increasing doses of dicumarol for 24 h. This corresponds to the right panel, where

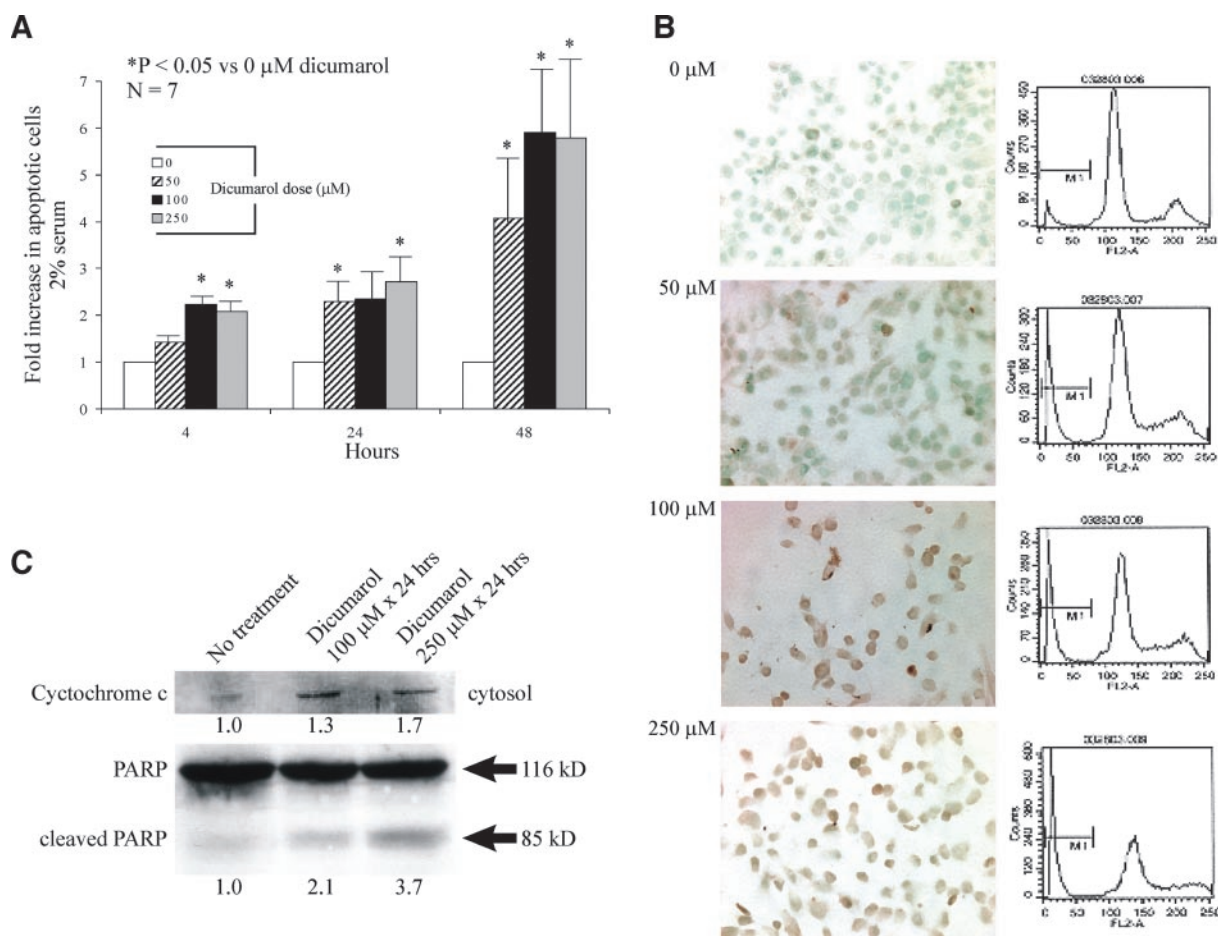


Fig. 2 A, dicumarol increased the percentage of apoptotic cells in a time-dependent and dose-dependent manner as measured by flow cytometry. MIA-PaCa-2 cells treated with dicumarol (0–250 μM) for 4, 24, 48, and 72 h were fixed and stained with propidium iodide. Cell cycle analysis was performed by flow cytometry. Apoptotic cells were estimated by calculating the number of subdiploid cells in the cell cycle histogram. $*P < 0.05$ versus 0 mM dicumarol, $n = 7$. B, dicumarol increased the percentage of apoptotic cells in a time-dependent and dose-dependent manner as measured by 3,3'-diaminobenzidine staining and flow cytometry. *Left panel*: MIA-PaCa-2 cells treated with dicumarol (0–250 μM) for 4, 24, 48, and 72 h and then stained with 3,3'-diaminobenzidine. Cells were counterstained with methyl green and were photographed under light microscopy. *Right panel*: apoptotic cells were estimated by calculating the number of subdiploid cells in the cell cycle histogram. Results are representative of three separate experiments. C, dicumarol increases cytochrome *c* release from the mitochondria into the cytosol in MIA PaCa-2 cells. Cells were treated with 100 and 250 μM dicumarol for 24 h, and cytosolic fractions were extracted. Thirty μg of cytosolic protein extracts from each sample were separated on a 15% SDS-PAGE and immunoblotted with monoclonal cytochrome *c* antibody. Data represent results from three separate experiments. Dicumarol increases poly(ADP-ribose) polymerase (PARP) cleavage in MIA PaCa-2 cells. Cells were treated with 100 and 250 μM dicumarol for 24 h, and equal amounts of protein were separated on 15% SDS-PAGE and immunoblotted. The M_r 116,000 band represents intact PARP, and the M_r 85,000 band represents the cleaved PARP. Data represent results from three separate experiments. The area of the bands relative to no treatment as measured by densitometric analysis is shown at the bottom of the lanes; these numbers indicate the relative amount of immunoreactive protein.

the number of apoptotic cells also increased with increasing doses of dicumarol. For example, the number of apoptotic cells increased from 5.5% in the controls to 19.2, 22.6, and 31.6% with dicumarol 50, 100, and 250 μM , respectively.

Dicumarol Induces Cytochrome *c* Release and PARP Cleavage. Cytochrome *c* is released from the mitochondria to the cytosol during apoptosis when mitochondrial membrane permeability is disrupted. Cytochrome *c* protein was present and unchanged in MIA PaCa-2 cells treated with dicumarol for 4 h at doses of 0, 50, 100, and 250 μM (data not shown). However, there was an increase in cytochrome *c* protein when cells were treated with dicumarol for 24 h at doses of 100 and 250 μM when compared with cells receiving no dicumarol (Fig. 2C).

Once cytochrome *c* is released from the mitochondria, it complexes with apoptotic protease-activating factor 1 to activate caspase-9. Once caspase-9 is activated, it can additionally activate downstream caspases such as caspase-3. During apoptosis, caspase-3 is cleaved into active caspase-3 (38). Activated caspase-3 in turn cleaves its substrate PARP from a M_r 116,000 protein to produce a M_r 85,000 fragment (39). As seen with cytochrome *c*, there were no changes in PARP immunoreactive protein in MIA PaCa-2 cells treated with dicumarol for 4 h at doses of 0, 50, 100, and 250 μM (data not shown). However, there was increased PARP cleavage in MIA PaCa-2 cells treated with dicumarol for 24 h at doses of 100 and 250 μM when compared with cells receiving no dicumarol (Fig. 2C).

Dicumarol-Induced Oxidative Stress as Measured by Thiol Analysis. Oxidative stress is commonly accompanied by increases in steady-state levels of oxidized thiols such as GSSG. Fig. 3 indicates that oxidative stress is induced by dicumarol in pancreatic cancer cells as evidenced by a disruption in glutathione metabolism leading to both increased steady-state levels of glutathione and GSSG. This was determined by measuring the intracellular concentrations of GSSG and total glutathione (reduced glutathione + GSSG) as an index of oxidative stress during dicumarol treatment. Fig. 3 shows that total and reduced glutathione concentrations were increased after 24 h of 50 and 100 μM dicumarol. This suggests that glutathione synthesis was induced by dicumarol during the same time frame as cytotoxicity was occurring. Fig. 3 also shows a significant increase in the steady-state levels of GSSG induced by 4- and 24-h treatment with 50 and 100 μM dicumarol. These results are consistent with the hypothesis that dicumarol-induced intracellular oxidative stress occurs during the same time frame as cytotoxicity and alterations in apoptotic pathways.

Intratumoral Injections of Dicumarol in Established Pancreatic Tumor Heterotopic Xenografts. To determine whether dicumarol would inhibit tumor cell growth *in vivo*, 2×10^6 MIA PaCa-2 cells were injected s.c. in the flanks of nude mice and allowed to grow for 15 days before treatment. Mean tumor volume growth was reduced in the MIA PaCa-2 cells when 100 μl of dicumarol (50, 100, and 250 μM) was injected into the s.c. tumors (Fig. 4A). The estimates for the slopes by group are provided in Table 1. Tumor volume was compared among the four groups using the data from days 1 through 28 only. For the animals that died before day 28, the last tumor volume was carried forward. To compare the treatment groups over time for tumor volume, the linear mixed model analysis (34) was used. In the linear mixed model analysis, group was

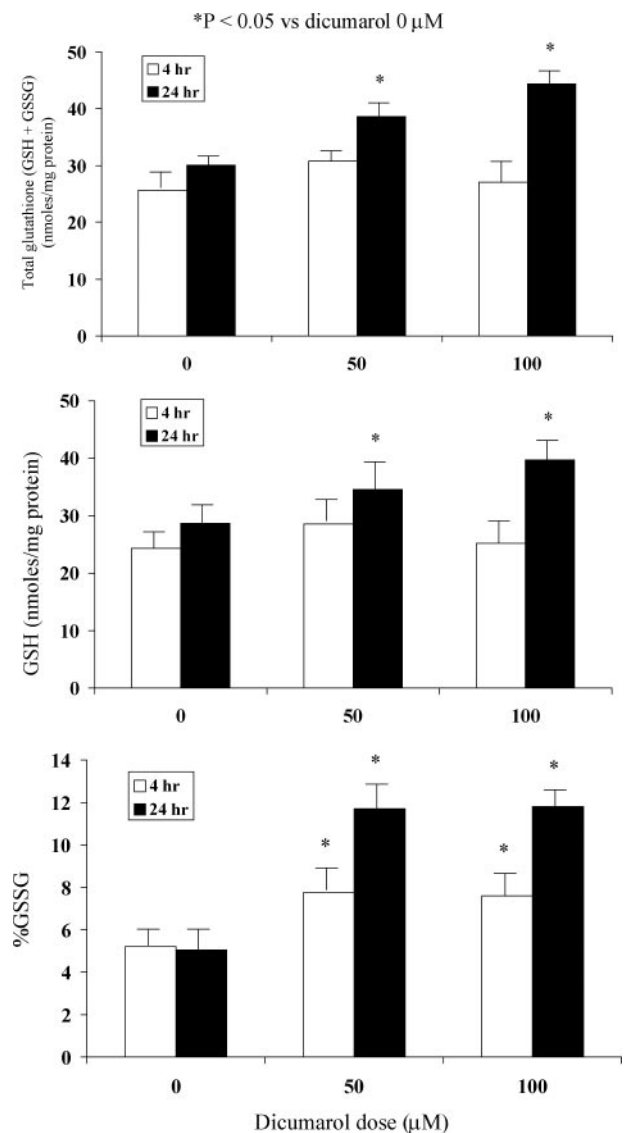


Fig. 3 Dicumarol results in oxidative stress as evidenced by disruption in glutathione metabolism. The effect of dicumarol (0, 50, 100, and 250 μM) on total, reduced glutathione (GSH), and oxidized glutathione [glutathione disulfide (%GSSG)] content in 4- and 24-h control and dicumarol-treated MIA PaCa-2 cells. Cells were harvested for glutathione analysis using spectrophotometric recycling assay. * $P < 0.05$ versus 0 μM dicumarol; means \pm SE, $n = 3$.

considered a fixed effect, and day was considered a continuous covariate. An interaction term between day and group was also included in the model. Using day as a continuous covariate assumes that the mean tumor volume is a linear function of days. The linear assumption was acceptable given that the adjusted R-squares were all >0.65 (group 1: adjusted $R^2 = 0.95$; group 2: adjusted $R^2 = 0.83$; group 3: adjusted $R^2 = 0.90$; group 4: adjusted $R^2 = 0.66$). Because of the large number of time points (11) and the small number of subjects/group (five to six), the possible covariance structures were limited. On the basis of the Akaike's Information Criterion (35), the compound symmetry covariance structure (Akaike's Information Criterion = 3037.9)

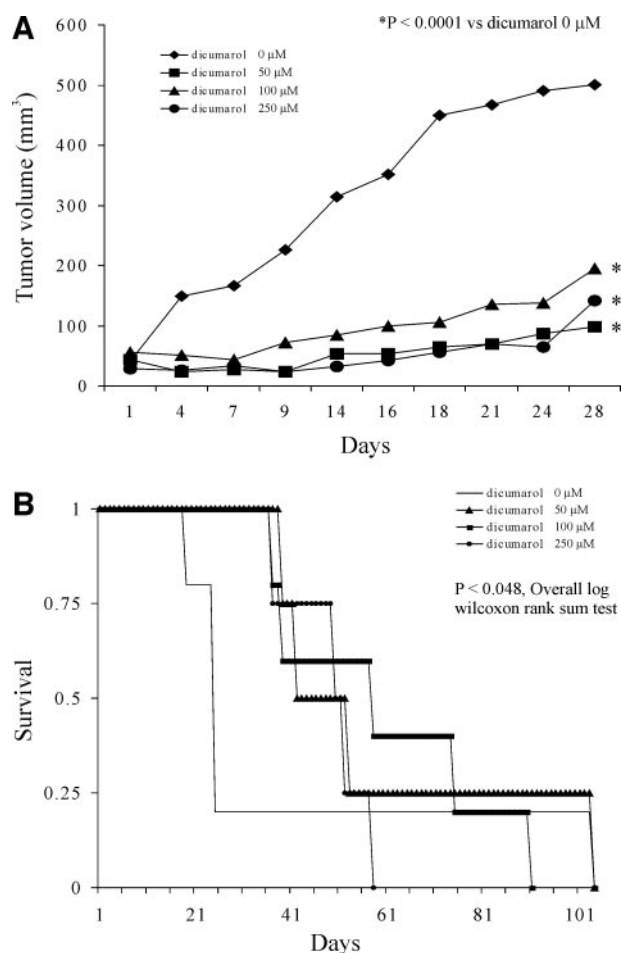


Fig. 4 A, single intratumoral injections of dicumarol (50, 100, and 250 μM) decreased MIA-PaCa-2 tumor growth in nude mice when studied out to 28 days after injection. Dicumarol-treated groups (50, 100, and 250 μM) exhibited a 2.5–5-fold decrease in tumor growth over no treatment (0 μM). Day 28: median tumor volume 501 mm^3 in control tumors (0 μM dicumarol) versus 98 mm^3 in tumors with one intratumoral injection of dicumarol (50 μM). Means, $n = 5\text{--}7/\text{group}$. B, intratumoral injections of dicumarol increased survival in pancreatic tumor xenografts. Kaplan-Meier plots of estimated survival after injection of MIA PaCa-2 tumors in nude mice. Single dose intratumoral injections of dicumarol (50, 100, and 250 μM) resulted in increased time to sacrifice when compared with control group (0 μM dicumarol; $P < 0.05$).

was selected instead of the autoregressive order 1 covariance structure (Akaike's Information Criterion = 3096.1). Therefore, to compare the treatment groups over time for tumor volume, the linear mixed model analysis assuming a compound symmetry covariance structure for within subjects was used. The linear mixed model suggested that the interaction between day and group was significant ($P < 0.0001$), *i.e.*, there is a significant difference among the groups in the slopes for tumor volume over time. The estimates for the slopes by group are provided in the Table 1. For example, tumor volumes were significantly reduced from $500 \pm 401 \text{ mm}^3$ in the controls to $195 \pm 172 \text{ mm}^3$ in tumors that had a single injection of dicumarol 100 μM ($P < 0.001$ versus controls, means \pm SD).

Kaplan-Meier plot for survival in animals receiving 0, 50, 100, and 250 μM dicumarol indicated that overall there were significant differences in survival (Fig. 4B). For example, on day 25 after injection, only 20% of control animals were alive, whereas 100% of animals receiving dicumarol (50, 100, or 250 μM) were living. Animals that received dicumarol (50 μM) as a single injection had the greatest effect on survival ($P < 0.04$) compared with animals that received vehicle alone (0 μM dicumarol).

DISCUSSION

Our study demonstrates that dicumarol decreases cell viability and clonogenic survival in a time-dependent and dose-dependent manner. Dicumarol increased the percentage of apoptotic cells in a time-dependent and dose-dependent manner as measured by DAB staining and flow cytometry, which was associated with cytochrome *c* release and PARP cleavage. Dicumarol also induced oxidative stress as evidence by disruption in glutathione metabolism. In established orthotopic pancreatic tumor xenografts, intratumoral injections of dicumarol slowed tumor growth and extended survival. Thus, the inhibition of NQO₁ with dicumarol induces cell killing, oxidative stress, and may prove to be useful in pancreatic cancer treatment.

Our study correlates with recent studies demonstrating that other inhibitors of flavoprotein oxidoreductases induce mitochondrial superoxide production leading to cytochrome *c* release, caspase activation, and apoptosis (27). Dicumarol, a specific inhibitor of the flavoprotein oxidoreductase NQO₁, also leads to increased reactive oxygen species. NQO₁, which detoxifies quinone xenobiotics, serves as a protective mechanism against reactive oxygen species and is elevated 12-fold in pancreatic cancer (24). Using NAD(P)H, NQO₁ directly reduces the quinone form to the hydroquinone form, thus bypassing the reactive semiquinone intermediate. Dicumarol inhibits NQO₁, causing increased production of reactive oxygen species when reactive semiquinones redox cycle, resulting in superoxide formation. Collectively, these studies demonstrate that reactive oxygen species play an important role in apoptosis and inhibition of NQO1 may be an important pathway to induce oxidative stress and subsequent cytotoxicity of quinones.

Pancreatic adenocarcinoma is now the fourth leading cause of cancer death in the United States with an overall 5-year survival rate of $<5\%$ (40). Even after curative resection, the 5-year survival rates achieved at specialized centers are $<20\%$, and the majority of patients die of metastatic cancer recurrence (41). Other adjuvant treatments such as radiation therapy and chemotherapy have not improved long-term survival after resection. Surgical resection of the primary tumor remains the

Table 1 *In vivo* tumor volume slopes over time for the data shown in Fig. 4A

Group	Slope (95% confidence interval)
Control	18.6 (15.2–22.0)
Dicumarol (50 μM)	2.6 (–1.1–6.3)
Dicumarol (100 μM)	5.1 (1.4–8.8)
Dicumarol (250 μM)	3.1 (–0.2–6.5)

only potentially curative treatment for pancreatic cancer, leading a number of investigators to study preoperative chemoradiation for its ability to convert locally unresectable pancreatic cancer to resectable disease. In an earlier study of 16 patients who had locally advanced, unresectable pancreatic cancer treated with preoperative chemoradiation therapy to enhance resectability, only 2 patients were able to undergo resection (42). A similar study by White *et al.* (43) with 25 patients noted that only 8% of patients with locally advanced pancreatic cancer treated with preoperative chemoradiation were able to undergo complete resection with negative margins. Thus, it is unlikely that neoadjuvant chemoradiation can convert unresectable lesions to resectable ones and thereby increase the number of patients who can be cured with combined-modality therapy. Our study presents an attractive alternative in the treatment of pancreatic tumors that at first seem unresectable by intratumoral injections of dicumarol to reduce tumor size.

Our study also correlates with other studies demonstrating that dicumarol-induced cytotoxicity via inhibition of NQO₁ can be enhanced with exogenous quinones like menadione (44). Previous studies have demonstrated that enhancement of menadione-mediated proteolysis by dicumarol suggests that the hydroquinone form of menadione is a nontoxic species or is rapidly conjugated and excreted from the cell and does not activate a cell death pathway (45). In nude mouse models of pancreatic cancer, antitumor quinones, including mitomycin C and doxorubicin analogues, have demonstrated inhibition of growth (46, 47). Additionally, oxidative stress induced by redox cycling of vitamins C and K₃ (menadione) have demonstrated *in vitro* tumor growth inhibition and increased survival of tumor bearing mice (48). This suggests the possibility that dicumarol combined with quinones could enhance pancreatic cancer treatment.

NQO₁ appears to be an important determinant of dicumarol toxicity because intratumoral injections of the drug resulted in slower tumor growth and increased survival with no recognized systemic toxicity. The intratumoral delivery of dicumarol presents an attractive alternative to decrease the systemic anticoagulant side effect. Additionally, dicumarol cytotoxicity may be additive or synergistic with other treatment modalities that increase reactive oxygen species, including ionizing radiation (49), altering antioxidant-detoxifying capacity (50), or glucose deprivation (51, 52). Future studies are planned to investigate combining therapies in multimodality treatment to obtain the maximal benefit of dicumarol.

In summary, dicumarol appears to induce oxidative stress and pancreatic cancer cell cytotoxicity, as well as apoptosis in a time-dependent and dose-dependent manner. Intratumoral injections of dicumarol slowed tumor growth and extended survival. Because other adjuvant treatments such as radiation therapy and chemotherapy have not improved long-term survival after resection, the inhibition of NQO₁ with dicumarol may prove to be useful in pancreatic cancer treatment.

REFERENCES

- Madari H, Panda D, Wilson L, Jacobs R. Dicumarol: a unique microtubule stabilizing natural product that is synergistic with Taxol. *Cancer Res* 2003;63:1214–20.
- Keating GJ, O’Kennedy R. The chemistry and occurrence of coumarins. In: O’Kennedy R, Thornes RD, editors. *Coumarins: biology, applications and mode of action*. West Sussex, United Kingdom: John Wiley & Sons; 1997. p. 23–64.
- Marshall ME, Mohler JL, Edmonds K, et al. An updated review of the clinical development of coumarin (1,2-benzopyrone) and 7-hydroxycoumarin. *J Cancer Res Clin Oncol* 1994;120:39–42.
- Moran E, Prosser E, O’Kennedy R, Thornes RD. The effect of coumarin and 7-hydroxycoumarin on the growth of human tumor cell lines. *J Irish Coll Phys Surg* 1993;22:41–8.
- Siegers CP, Bostelmann HC. Effect of coumarin on cell cycle proliferation in human tumor cell lines. *J Irish Coll Phys Surg* 1993;22:47–50.
- Myers RB, Parker M, Grizzle WE. The effects of coumarin and suramin on growth of malignant renal and prostatic cell lines. *J Cancer Res Clin Oncol* 1994;120:11–3.
- Finn GJ, Creaven B, Egan DA. Study of the *in vitro* cytotoxic potential of natural and synthetic coumarin derivatives by using human normal and neoplastic skin cell lines. *Melanoma Res* 2001;11:461–7.
- Brar SS, Kennedy TP, Whorton AR, et al. Reactive oxygen species from NAD(P)H: quinone oxidoreductase constitutively activate NF-kappaB in malignant melanoma cells. *Am J Physiol* 2001;280:C659–76.
- Feuer G, Kellen JA, Kovacs K. Suppression of 7,12-dimethylbenz(a)anthracene-induced breast carcinoma by coumarin in the rat. *Oncology* 1976;33:35–9.
- Thornes D, Daly L, Lynch G, et al. Prevention of early recurrence of high risk malignant melanoma by coumarin. *Eur J Surg Oncol* 1989;15:431–5.
- Omarbasha B, Fair WR, Heston WD. Effect of coumarin on the normal rat prostate and on the R-3327H prostatic adenocarcinoma. *Cancer Res* 1989;49:3045–9.
- Raev LD, Voinovea E, Ivanov IC, Popov D. Antitumor activity of some coumarin derivatives. *Pharmazie* 1990;45:696.
- Maucher A, Von Angerer E. Antitumor activity of coumarin and 7-hydroxycoumarin against 7,12-dimethylbenz[a]anthracene-induced rat mammary carcinomas. *J Cancer Res Clin Oncol* 1994;120:502–4.
- Thornes RD, Daly L, Lynch G, Breslin B, Browne H, Browne HY, Corrigan T, Daly P, Edwards G, Gaffney E. Treatment with coumarin to prevent or delay recurrence of malignant melanoma. *J Cancer Res Clin Oncol* 1994;120:S32–4.
- Marshall ME, Bulter K, Fried A. Phase I evaluation of coumarin (1, 2-benzopyrone) and cimetidine in patients with advanced malignancies. *Mol Biother* 1991;3:170–8.
- Mohler JL, Gomella LG, Crawford ED, et al. Phase II evaluation of coumarin (1,2-benzopyrone) in metastatic prostatic carcinoma. *Prostate* 1992;20:123–31.
- Smith GF, Neubauer BL, Sundboom JL, et al. Correlation of the *in vivo* anticoagulant, antithrombotic and antimetastatic efficacy of warfarin in the rat. *Thromb Res* 1988;50:163–74.
- Dinkova-Kostova AT, Talalay P. Persuasive evidence that quinone reductase type 1 (DT-Diaphorase) protects cells against the toxicity of electrophiles and reactive forms of oxygen. *Free Rad Biol Med* 2000; 29:231–40.
- Brar DD, Kennedy TP, Whorton AR, Murphy TM, Chitano P, Hoidal JR. Requirement for reactive oxygen species in serum-induced and platelet-derived growth factor-induced growth of airway smooth muscle. *J Biol Chem* 1999;274:20017–26.
- Hollander PM, Ernster L. Studies on the reaction mechanism of DT diaphorase. Action of dead-end inhibitors and effects of phospholipids. *Arch Biochem Biophys* 1975;169:560–7.
- Josoda S, Nakamura W, Hayashi K. Properties and reaction mechanisms of DT diaphorase from rat liver. *J Biol Chem* 1974;249: 6416–23.
- Duthie SJ, Grant MH. The role of reductive and oxidative metabolism in the toxicity of mitoxantrone, adriamycin and menadione in human liver derived Hep G2 hepatoma cells. *Br J Cancer* 1989;60: 566–71.

23. Cullen JJ, Hinkhouse MM, Grady M, et al. Dicumarol inhibition of NAD(P)H:quinone oxidoreductase (NQO₁) induces growth inhibition of pancreatic cancer via a superoxide-mediated mechanism. *Cancer Res* 2003;63:5513–20.
24. Logsdon CD, Simeone DM, Binkley C, et al. Molecular profiling of pancreatic adenocarcinoma and chronic pancreatitis identifies multiple genes differentially regulated in pancreatic cancer. *Cancer Res* 2003;63:2649–57.
25. Siegel D, Ross D. Immunodetection of NQO1 in human tissues. *Free Radic Biol Med* 2000;29:246–53.
26. Larm JA, Vaillant F, Linnane AW, Lawen A. Up-regulation of the plasma membrane oxidoreductase as a prerequisite for the viability of human Namalwa ρ^0 cells. *J Biol Chem* 1994;269:30097–100.
27. Li N, Ragheb K, Lawler G, et al. DPI induces mitochondrial superoxide-mediated apoptosis. *Free Radic Biol Med* 2003;34:465–77.
28. Edlund C, Elhammer A, Dallner G. Distribution of newly synthesized DT-diaphorase in rat liver. *Biosci Rep* 1982;2:861–5.
29. Winski SL, Koutalos Y, Bentley DL, Ross D. Subcellular localization of NAD(P)H:quinone oxidoreductase 1 in human cancer cells. *Cancer Res* 2002;62:1420–4.
30. Anderson ME. Tissue glutathione. In: Greenwald RA, editor. *Handbook of methods for oxygen radical research*. Boca Raton, FL: CRC Press; 1985. p. 317–23.
31. Griffith OW. Determination of glutathione and glutathione disulfide using glutathione reductase and vinylpyridine. *Anal Biochem* 1980;106:207–12.
32. Lowry OH, Rosenbrough NG, Farr AL, Randall RJ. Protein measurement using the folin phenol reagent. *J Biol Chem* 1951;193:265–75.
33. Wydert C, Roling B, Liu J, Ritchie JM, Oberley LW, Cullen JJ. Suppression of the malignant phenotype in human pancreatic cancer cells by the overexpression of manganese superoxide dismutase. *Mol Cancer Ther* 2003;2:361–9.
34. Littell RC, Milliken GA, Stroup WW, Wolfinger RD, editors. *SAS system for mixed models*. SAS Institute Inc.: Cary, NC; 1996.
35. Akaike H. Information theory and an extension of the maximum likelihood principle. In: Petrov BN, Csaki F, editors. *Second international symposium on information theory*. Akademiai Kiado: Budapest, Hungary; 1973. p. 267–81.
36. Hulse M, Feldman S, Bruckner JV. Effect of blood sampling schedules on protein drug binding in the rat. *J Pharmacol Exp Ther* 1981;218:416–20.
37. Preusch PC, Siegel D, Givson NW, Ross D. A note on the inhibition of DT-diaphorase by dicoumarol. *Free Radic Biol Med* 1991;11:77–80.
38. Nicholson DW, Ali A, Thornberry NA, et al. Identification and inhibition of the ICE/CED-3 protease necessary for mammalian apoptosis. *Nature (Lond.)* 1995;371:37–43.
39. Lazebnik YA, Kaufmann SH, Desnoyers S, Poirier GG, Earnshaw WC. Cleavage of poly(ADP-ribose) polymerase by a proteinase with properties like ICE. *Nature (Lond.)* 1994;371:346–7.
40. Jemal A, Thomas A, Murray T, Thun M. *Cancer statistics, 2002*. *CA - Cancer J Clin* 2002;52:23–47.
41. Yeo CJ, Cameron JL. Pancreatic cancer. *Curr Probl Surg* 1999;36:59–152.
42. Jessup JM, Steele G, Mayer RJ, et al. Neoadjuvant therapy for unresectable pancreatic adenocarcinoma. *Arch Surg* 1993;128:559–64.
43. White R, Lee C, Anscher M, et al. Preoperative chemoradiation for patients with locally advanced adenocarcinoma of the pancreas. *Ann Surg Oncol* 1999;6:38–45.
44. Pink JJ, Planchon SM, Tagliarino C, Varnes ME, Siegel D, Boothman DA. NAD(P)H:quinone oxidoreductase activity is the principal determinant of β -lapachone cytotoxicity. *J Biol Chem* 2000;275:5416–24.
45. Wefers H, Sies H. Hepatic low-level chemiluminescence during redox cycling of menadione and the menadione-glutathione conjugate: relation to glutathione and NAD(P)H:quinone reductase (DT-diaphorase) activity. *Arch Biochem Biophys* 1983;224:568–78.
46. An Z, Wang X, Kubota T, Moossa AR, Hoffman RM. A clinical nude mouse metastatic model for highly malignant human pancreatic cancer. *Anticancer Res* 1996;16:627–31.
47. Szepeshazi K, Schally AV, Halmos G, et al. Targeting of cytotoxic somatostatin analog AN-238 to somatostatin receptor subtypes 5 and/or 3 in experimental pancreatic cancers. *Clin Cancer Res* 2001;7:2854–61.
48. Calderon PB, Cadrobbi J, Marques C, et al. Potential therapeutic application of the association of vitamins C and K₃ in cancer treatment. *Curr Med Chem* 2002;9:2271–85.
49. Lin X, Zhang F, Bradbury CM, et al. 2-Deoxy-D-glucose-induced cytotoxicity and radiosensitization in tumor cells is mediated via disruptions in thiol metabolism. *Cancer Res* 2003;63:3413–7.
50. Darby Weydert CJ, Smith BJ, Xu L, et al. Inhibition of oral cancer cell growth by adenovirus MnSOD plus BCNU treatment. *Free Radic Biol Med* 2003;34:316–29.
51. Lee YJ, Galoforo SS, Berns CM, et al. Glucose deprivation-induced cytotoxicity and alterations in mitogen-activated protein kinase activation are mediated by oxidative stress in multidrug-resistant human breast carcinoma cells. *J Biol Chem* 1998;273:5294–9.
52. Blackburn RV, Spitz DR, Liu X, et al. Metabolic oxidative stress activates signal transduction and gene expression during glucose deprivation in human tumor cells. *Free Radic Biol Med* 1999;26:419–30.